CONF-780408--2

EXPERIMENTAL STUDY OF AMMONIA CONDENSATION ON VERTICAL FLUTED TUBES*

S. K. Combs
Engineering Technology Division
Oak Ridge National Laboratory
Oak Ridge, Tennessee 37830

MASTER

ABSTRACT

Experiments were run to determine heat transfer performance of single vertical tubes with ammonia condensing on the outside. The four test tubes (aluminum) were of 1-in. nominal diameter and 4-ft length with 0 (smooth), 24, 48, and 60 external flutes. The condensing heat transfer coefficients are reported as composite coefficients that include the resistance of both the condensing side and the tube wall. The composite condensing coefficients ranged from 720 to 9600 Btu/hr·ft^2·°F over a heat flux range of 1600 to 16000 Btu/hr·ft^2. All parameters were based on total condensing surface area. The data show that, for a given heat flux, a fluted tube can increase condensing coefficients up to 7.2 times smooth tube values. Corresponding condensing temperature differences (composite) ranged from 0.3 to 23°F in the experiments; and the data show that, for a given condensing temperature difference, a fluted tube can accommodate heat loads up to 5.4 times the smooth tube values. Conversely, for a given heat load, a smooth tube requires condensing temperature differences up to 9.7 times the fluted tube values.

NOMENCLATURE

a_o	y-intercept on the Wilson plot
a_1	slope of the line on the Wilson plot
A	heat transfer surface area of test tube
c_p	specific heat
D	tube diameter
g	local gravitational acceleration
h	average or mean individual heat transfer coefficient
h_{fg}	latent heat of vaporization
h*	composite condensing heat transfer coefficient including both vapor side and wall
H	standard nondimensional heat transfer coefficient (average or mean)

*Research sponsored by the Department of Energy under contract with Union Carbide Corporation.

EAB

DISCLAIMER

k	thermal conductivity
$\dot{m}$	mass flow rate
P	pressure
Q	heat load
Q/A	heat flux
r	radius
R	resistance to heat flow
$R_{\Delta T^*}$	ratio of condensing temperature differences [ΔT^* (smooth tube)/ ΔT^* (fluted tube)] at equal heat load
R_{h^*}	ratio of condensing coefficients [h^* (fluted tube)/h^* (smooth tube)] at equal heat flux
R_Q	ratio of heat loads [Q (fluted tube)/Q (smooth tube)] at equal condensing temperature difference
Re	Reynolds number
T	temperature
ΔT	temperature difference
$\overline{\Delta T}$	mean temperature difference between the condensing vapor and coolant
ΔT^*	composite condensing temperature difference including both vapor side and wall
U	overall condensing heat transfer coefficient
v	water velocity

Greek Symbols

Γ	Condensate mass flow rate at bottom of tube per unit length of periphery
μ	absolute viscosity
ρ	mass density
σ	surface tension

Subscripts

avg	average
fi	inside fouling
fo	outside fouling
i	inside
o	outside
v	vapor; vapor (condensing) side
w	water; water side
wall	wall; surface

INTRODUCTION

One method for increasing the thermal performance of heat exchangers is enhancement of the heat transfer coefficient through use of modified heat transfer surfaces. Studies at the Oak Ridge National Laboratory [1] in the period 1964 to 1972 considered the thermal performance of evaporator-condenser tubes modified in various ways to augment condensation and evaporation or boiling coefficients. This work was done for the Office of Saline Water and concentrated on water and brines for application to desalination plants. The results from the program were very encouraging, reporting overall coefficients up to seven times larger for augmented surfaces than those obtained with conventional smooth tubes.

In a manner similar to this earlier work, the present study examined the potential for improving the heat transfer performance of condensers for conditions typified by an ocean thermal energy conversion (OTEC) plant. Any significant increase in the thermal performance of the heat exchangers (condensers and evaporators) could result in a substantial capital cost reduction of a power conversion plant for utilizing the resource and favorably affect the overall feasibility of developing the resource.

Specifically, the enhancement of heat transfer coefficients for ammonia condensing on vertical tubes was investigated in this study. Ammonia was chosen since this is the prime candidate for the working fluid in an OTEC plant. The need for these studies rests in large part on the sparseness of the condensing experimental data for fluids other than water. The experimental study undertaken included the determination of average heat transfer coefficients for ammonia condensing both on smooth tubes and on fluted tubes of various geometries. The emphasis on fluted tubes stemmed from the performance efficacy identified in water studies, such as that of Alexander and Hoffman [1].

BACKGROUND

In 1916, Nusselt [2] derived the theoretical relations for predicting heat transfer coefficients for film condensation of pure vapors on tubes and plates. Subsequently, extensive work was carried out in the general area of film condensation by other investigators; their efforts included many modifications to Nusselt's analysis. Thus, for film condensation on the outside of vertical surfaces in laminar flow, McAdams [3] developed a semiempirical relationship for predicting the heat transfer coefficients in which Nusselt's theoretical equation was multiplied by a constant. This recommended equation by McAdams was based on a comparison of Nusselt's predicted coefficients with experimental data; the expermental data averaged at least 20% above Nusselt's theoretical prediction. Kutateladze [4] presented a semiempirical equation for predicting film condensation coefficients for laminar flow on vertical surfaces that purports to account specifically for the effect of ripples (irregularities in the liquid-vapor interface) on heat transfer. For film condensation where the flow is turbulent, McAdams [3] recommended the correlation of Kirkbride [5].

More recently, investigators have focused their attention on the potential for augmenting film condensation heat transfer. In most film-type condensing situations, the major resistance to heat transfer lies in the liquid film that forms on the cooled surface as the vapor condenses. Therefore, condensation heat transfer enhancement depends primarily on methods for reducing the effective thickness (or resistance) of this liquid film. Modified surfaces, such as fluted tubes, have proved successful in reducing the resistance of the liquid film.

The first study of fluted enhanced surfaces was by Gregorig [6] in 1954, who showed analytically and experimentally that fluting the tube surface can significantly augment film condensation heat transfer; thus, by fluting the outside surface of a vertical tube, Gregorig obtained increases of 200 to 800% in the average film condensation coefficient for condensing steam. The observed enhancement was attributed to surface tension forces (see Fig. 1 for illustration of fluted tube principle of operation) acting to push the condensate from the convex surfaces (crests) into the concave channels (troughs) down which it drains by gravity. This results in thinning of the liquid film on the crests, greatly reducing the resistance to heat flow through the crest area. The resistance to heat flow is increased somewhat in the troughs through thickening of the film by addition of the fluid from the crests. The overall effect is an improvement in the average condensing film coefficient; however, the magnitude of the augmentation depends on the trade off between improvement in the crest area heat transfer and the degradation in trough area heat transfer.

Gregorig's idea stemmed from the fact that the pressure of the fluid inside a curved interface will be greater than the pressure of the fluid outside the interface by an amount given by Laplace's formula [7]:

$$P_1 - P_2 = \sigma(1/r_1 + 1/r_2) \ , \qquad (1)$$

where $(P_1 - P_2)$ is the surface pressure difference, r_1 and r_2 are the principal radii of curvature of the interface, and σ is the surface tension. Thus, if a vertical condensing surface is not smooth, but instead contains corrugations or ridges (flutes) and troughs running vertically on the surface, condensate forming on the crests will be at a slightly higher pressure than surrounding vapor, while liquid in the troughs will be slightly below the pressure of the vapor. This difference in pressure is what forces the liquid off the crests into the troughs resulting in thin film regions as illustrated in Fig. 1.

Other investigators have confirmed Gregorig's findings. The study of fluted tubes by Carnavos [8] reported film condensing coefficients 4.5 to 7 times greater than those obtained for a comparable smooth tube at a given heat flux. The work of Alexander and Hoffman [1] with modified surfaces indicated significant increases in the overall heat transfer coefficients (6 to 7 times larger than those of smooth tubes); no direct measurement of condensing-side coefficients were made in this study. Thomas [9,10] achieved considerable enhancement of film condensation by modifying vertical condenser tubes in two ways: (1) loosely attached small longitudinal wires and (2) loosely clamped longitudinal fins. With the wires, Thomas was able to increase the condensing film heat transfer coefficient as much as a factor of 4.5 over a smooth tube; while with the fins, enhancement factors greater than 9 were reported.

All of the work previously mentioned was with condensing steam and, in general, most of the work on film condensation has been done with steam. Little experimental data are reported for fluids other than water, and even less for such fluids condensing on enhanced surfaces. Thus, for the past several years, the Oak Ridge National Laboratory [11,12] has been involved in an experimental program to obtain film heat transfer coefficients for fluorocarbons condensing on both smooth and fluted vertical surfaces. Kratz et al. [13] studied ammonia condensing on smooth tubes in several types of condensers, but reported only overall coefficients.

EXPERIMENTAL EQUIPMENT

Equipment used in this investigation is shown schematically in Fig. 2. The system was designed for a heat load of 5 kW and consisted of three circuits — an ammonia loop, a primary cooling loop, and a secondary cooling loop. The ammonia loop was designed for a maximum operating pressure and temperature of 250 psia and 110°F. The test section, a single-tube vertical condenser, was built to accommodate tubes of 1- or 2-in. nominal diameter and 4 ft in length. The system was manually controlled, and the heat load was set by the power input to the boiler. The ammonia loop was constructed of stainless steel to minimize compatibility problems. View ports on the test section permitted visual observation of the condensing surface with the aid of a light at suitable locations. Water served as the coolant in both the primary and secondary cooling loops. The primary coolant removed the heat from the tube in the test section; and in turn, the heat was transferred to the secondary coolant.

General Flow Description

Flow directions in the system are indicated by arrows in Fig. 2. Typically, the ammonia was vaporized in the boiler and passed through an entrainment separator before entering the condensing test section. The vapor entered the top of the test section, and the liquid (collected in the separator) returned to the boiler. The vapor condensed on the outer surface of the test tube in the test section and formed a falling film of liquid. The liquid condensate exited at the bottom of the test section, passed through a condensate measuring station, and returned to the bottom of the boiler to complete the closed loop. A pump was not needed for the circulation of the ammonia since the liquid head in the test-section side of the loop furnished the driving force required for flow through the condensate measuring station.

In the primary cooling loop, a centrifugal pump transferred demineralized water from a storage tank to the bottom of the test section and upward through the test tube. The primary cooling flow was measured by rotameters upstream of the test section and controlled by a hand valve located downstream of the test section. From the top of the test section, the water returned to the storage tank to complete the closed loop. The secondary cooling loop removed the heat load from the system by transferring the heat from the primary cooling water to plant process water. Primary cooling water recirculating through the storage tank dumped heat to secondary cooling water which passed through a cooling coil in the tank and then discharged to the drain. The flow rate of the secondary coolant was regulated by a hand valve located downstream of the cooling coil.

Condensing Test Section

The shell of the test section was fabricated from 4-in. Schedule 40 stainless steel pipe. Figure 3 is a detailed sketch of the test section including an assembly diagram. The outside (condensing) surface of the experimental test tube could be viewed at locations near the top and bottom of the test tube through two windows (Fig. 3). Provision was made at the bottom of the test section to collect separately the condensate forming on the inside of the shell, and this condensate was returned to the boiler downstream of the condensate measuring station. The total condensing length in the test section was 4 ft.

A stainless steel rod of 0.50-in. outside diameter was installed through the center of the test section (inside the test tube) in order to decrease the hydraulic diameter and increase the velocity for a given primary cooling volume flow. Both of these variations tended to increase the heat transfer coefficients on the water side; and, as a result, improved the accuracy of the Wilson-plot technique [14] used to interpret the experimental data. For example, with a smooth 0.87-in.-ID tube (designated Tube A in the following section), insertion of the 0.50-in.-OD rod decreased the hydraulic diameter by 57% and increased the velocity by 49%.

Test Tubes

The performance of four tubes (1-in.-nominal diameter) was examined in this investigation. Letter designations (as noted in Table 1) are used to identify the tubes. Detailed descriptions of the tubes are given in Table 1. All tubes were aluminum and, with the exception of Tube A, were fluted; Tube A had a smooth surface. As shown in Table 1, Tubes F and G had rounded flutes (corrugations), while Tube E had square flutes (square ridges). All tubes except Tube G had a smooth inside surface; the inside surface of Tube G contained some irregularities (scratches) apparently created during the extrusion process.

Tube E was selected from an assortment of tubes remaining from previous heat transfer studies at the Oak Ridge National Laboratory by Alexander and Hoffman [1]. Tubes F and G were fortuitous findings, being commonly sold as standard shower curtain rods, in that the number of flutes fell conveniently in multiples of 12 between Tubes A and E. Tube F is distributed by the Macklanburg Duncan Company, and Tube G is distributed by Kirsch under the designation Part No. BF100-54. A duplicate of Tube F (designated as Tube F-1) was also tested with a neoprene skirt attached at the midpoint of the condensing length; these tests were conducted to obtain some indication of the effect of tube length on the condensing heat transfer performance of fluted tubes.

PROCEDURES AND INSTRUMENTATION

Heat rates and temperature differences in the test section were calculated from experimental data taken during steady-state operations. Accurate temperature measurements were critical, since it was sometimes necessary to measure very small temperature differences ($\sim$0.2°F) to within $\pm$0.04°F to obtain reliable heat balances. Further, small condensate flows (as low as 0.01 gpm) had to be measured accurately for good interpretation of the experimental data.

Steady-State Operation

The heat rate to the boiler was controlled manually by setting the voltage to the boiler. After setting the heat rate to the boiler, the primary cooling flow rate was adjusted by the valve downstream of the test section. Since the inlet temperature of the secondary cooling water was fixed by the plant process water conditions, the flow rate of the secondary cooling water was used to control the temperature of the primary cooling water. This, in turn, controlled the vapor temperature in the test section. Temperatures and pressures throughout the system were monitored to determine when steady-state conditions existed; steady state was assumed when there was no significant change in temperatures ($\pm$0.1 to $\pm$0.2°F) throughout the system over a five- to ten-minute span.

Once a steady state was achieved, the experimental data were recorded. The information recorded included the vapor temperature and pressure in both the condenser and boiler, the flow rate and temperature of the condensate, the inlet and outlet temperatures and flow rates of the primary and secondary coolants, and the voltage and current to the boiler. These experimental data were then used to calculate heat transfer rates and temperature differences in the system and to check pressure-temperature values against saturation data for ammonia.

After all the data were recorded for a given steady-state situation, the flow rate of the primary cooling water was changed and the flow rate of the secondary cooling water adjusted (range of 0 to 4 gpm) until the system reached a new steady state. When this steady state was reached, the experimental data were again recorded. The same procedure was followed until data were collected for at least three coolant flow rates at the same boiler heat rate. In the experiments, the primary cooling flow rates ranged from 3.0 to 34.0 gpm. The heat rate to the boiler was then changed, and the entire procedure was repeated at the new heat rate.

The major difficulty encountered during operation of the system arose from the presence of noncondensable gases (primarily air). Great care was taken to insure that noncondensables were removed before experimental data were recorded.

Temperature

The system was equipped with chromel-alumel thermocouples that were read with a potentiometer to obtain the temperatures used in the data analysis and recorded continuously on two multipoint recorders to obtain a permanent record. Thermocouples were located in the liquid and vapor of the boiler, in the vapor feed to the test section, in the inlet and outlet of both cooling water loops, near the condensate measuring station, and on each heater. The recorded thermocouple data were used in deciding when the system reached a steady state.

Both a quartz thermometer and a thermistor were located in the vapor feed to the test section and in the inlet and outlet of the primary cooling water. In addition, a quartz thermometer was located near the condensate measuring station. The information from the quartz thermometers (Hewlett Packard, Model 2801A) and the thermistors (Thermometrics, Part No. S-10-4-wire) were used for data reduction because of the greater accuracy attributed to these instruments. However, the

experimental data from the three sets of temperature measuring instruments were checked against each other to increase the confidence in the temperature measurements.

Condensate Flow Rate

The condensate flow in the ammonia loop was measured by two instruments: an integral orifice meter and a turbine flow transducer. These two instruments were located in parallel with piping permitting the routing of the flow through either device. An integral flow orifice assembly was used to adapt a pneumatic d/p cell transmitter (Foxboro Model 15A) for the measurement of low flow rates. With the integral orifice meter, it was necessary to change orifice plates (bores of 0.0595, 0.0810, 0.995, and 0.159 in.) for various flow ranges. A turbine flow transducer (Flow Technology, Model FTM-NX3-LJS) equipped with a range extending amplifier (Flow Technology, Model LFA-300AX) facilitated operation. The range extending amplifier made it possible to cover the full range of interest (0.01 to 0.2 gpm) with only one instrument. Measurements from the turbine flow transducer were used in reducing the data with the integral orifice meter results used as a check. The two values always agreed to within a few percent.

ANALYSIS

Overall Condensing Coefficients

The heat transfer rate in the condenser can be written:

$$Q = UA\overline{\Delta T} \ , \tag{2}$$

where U is the overall heat transfer coefficient, $\overline{\Delta T}$ is the mean temperature difference between the condensing vapor and the primary cooling water, and A is surface area of the test tube. The heat transfer rate can be computed from either the condensate mass flow rate ($\dot{m}_c$) or from the product of mass flow rate ($\dot{m}_w$) and temperature rise (ΔT_w) of the primary cooling water; thus,

$$Q = \dot{m}_c \, h_{fg} \tag{3}$$

and

$$Q = \dot{m}_w \, c_{pw} \, \Delta T_w \ , \tag{4}$$

where h_{fg} is the latent heat of ammonia, c_{pw} is the heat capacity of water. These two values provided a means for checking heat balances; for over 98% of the runs, the checks were better than +10% and over 80% were better than +5%. In this analysis, all physical property data for ammonia were taken from ASHRAE handbooks [15-18], where ammonia is designated as Refrigerant 717.

The arithmetic mean difference is used for $\overline{\Delta T}$, since in most cases the temperature difference across the water was relatively small. Therefore, assuming saturated vapor:

$$\overline{\Delta T} = T_v - T_{w,avg} \tag{5}$$

where T_v is the ammonia vapor temperature and $T_{w,avg}$ is the average water temperature. Defining an overall coefficient (U_o) based on the outside surface area (A_o) and rearranging Eq. (2):

$$U_o = \frac{Q}{A_o \overline{\Delta T}} \tag{6}$$

The next step in the analysis is the evaluation of individual condensing-side coefficients from the overall coefficients.

Individual Condensing-Side Coefficients

A technique introduced by Wilson [14] in 1915 was used as the primary method of analysis in this study; this is a graphical method of interpreting overall coefficients of heat transfer in surface condensers such that individual condensing-side coefficients can be evaluated. Beatty et al. [18] determined film coefficients for various fluids condensing on the outside of finned tubes by a modification of the method proposed by Wilson. In this analysis, the Wilson-plot method was applied as originally presented by Wilson. The following treatment presents the method and describes the application to the experimental data in this study.

The overall resistance to heat flow ($\Sigma R = 1/U$) in a condenser is equal to the sum of the individual resistances; thus,

$$1/U = R_v + R_{fo} + R_{wall} + R_{fi} + R_w , \tag{7}$$

where R_v is the resistance on the vapor (condensing) side, R_{wall} that of the wall, R_w that on the water side, and R_{fo} and R_{fi} account for any fouling on the outside and inside surfaces of the tube, respectively. Introducing individual average heat transfer coefficients (h), neglecting any fouling, and correcting for differences in area, the overall coefficient based on the outside surface area is represented by:

$$\frac{1}{U_o} = \frac{1}{h_v} + R_{wall} + \frac{A_o}{h_w A_i} , \tag{8}$$

where A_i is the inside surface area of the tube, h_v is the vapor-side heat transfer coefficient based on the outside tube area, and h_w is the water-side heat transfer coefficient based on the inside tube area. For a smooth tube, the wall resistance based on the outside tube area is given by:

$$R_{wall} = r_o \ln (r_o/r_i)/k , \tag{9}$$

where r_o and r_i are the outside and inside radii of the tube, respectively, and k is the thermal conductivity of the tube wall.

Neglecting the effects of changes in water temperature, the water-side resistance ($1/h_w$) can be taken as a function of the water velocity (v). For turbulent flow of water, this can be expressed as

$$1/h_w \propto 1/v^{0.8} ,$$

and thus, Eq. (8) can be rewritten:

$$\frac{1}{U_o} = \frac{1}{h_v} + R_{wall} + a_1 v^{-0.8} . \tag{10}$$

If, following Wilson, the sum of the first two resistances ($1/h_v + R_{wall}$) is taken as approximately constant, Eq. (10) becomes:

$$\frac{1}{U_o} = a_o + a_1 v^{-0.8} . \tag{11}$$

In this form, a plot of $1/U_o$ vs $1/v^{0.8}$ on ordinary rectangular coordinates should give a straight line from which the constants a_o and a_1 can be determined. Thus, the constant a_o is given by the y-intercept on the Wilson plot and corresponds to the sum of the first two resistances (vapor side plus wall) in Eq. (10):

$$a_o = \frac{1}{h_v} + R_{wall} . \tag{12}$$

The constant a_1 is the slope of the straight line on the Wilson plot.

For a smooth tube, Eq. (9) can be used to calculate a wall resistance, and h_v can be computed from Eq. (12). However, for fluted tubes, it is very difficult to estimate the contribution of the wall due to the more complicated wall geometry and heat distribution. Accordingly, the coefficients for the fluted tubes are reported as a composite condensing coefficient (h*) that includes both the vapor-side resistance and the wall resistance:

$$h^* = \frac{1}{(1/h_v) + R_{wall}} \tag{13}$$

or

$$h^* = \frac{1}{a_o} . \tag{14}$$

The corresponding composite condensing temperature difference is given by:

$$\Delta T^* = \frac{Q}{h^* A_o} , \tag{15}$$

and represents the temperature difference between the vapor and the inside wall of the test tube.

An alternative scheme was employed for a rough check of the Wilson-plot results. Heat transfer correlations for fully developed turbulent flow in round tubes — McAdams [3], Colburn [19], Sieder & Tate [20] — were used to estimate the water-side heat transfer coefficients. The composite coefficient was backed out of the overall coefficient by subtracting the estimated water-side coefficient. Substituting the water-side coefficient predicted by one of the three correlations for h_w in Eq. (8) and solving for the composite condensing coefficient yields:

$$h^* = \frac{1}{(1/U_o) - (A_o/h_w A_i)} \quad . \tag{16}$$

However, the composite coefficient estimated in this way is very sensitive to the water-side coefficient, especially at low water velocities (low water-side coefficients). Therefore, the scheme was only employed at the highest water velocity for each Wilson plot. Results from this scheme are presented in the next section.

The analyses outlined by Rohsenow and Choi [21] for the influence of fluid film turbulence and vapor shear stress on the condensate flow indicated negligible effect on the ammonia condensation results. The maximum vapor velocity in the test section during the experiments was less than 0.2 ft/sec. The assumption of no fouling is probably valid, since the tubes were run for only short periods of time (two to four weeks) during which the experimental overall coefficients did not degrade.

RESULTS AND DISCUSSION

Sample Wilson plots are shown in Figs. 4 and 5 for a smooth and a fluted tube, respectively. Results from the Wilson plots are presented in Fig. 6, where h^* (the composite condensing coefficient) is given as a function of the heat flux (Q/A); it should be noted that the heat transfer area used in obtaining both h^* and Q/A is the total outside tube surface area. Parameter ranges for the experiments were as presented in Table 2. A more detailed description of this study (including experimental data and sample calculations) is presented in Reference 22.

Smooth Tube

Tube A (smooth) data are presented in Fig. 7 in nondimensional form. The ordinate is the standard nondimensional heat transfer coefficient (mean or average coefficient):

$$H = h_v/(k^3\rho^2 g/\mu^2)^{1/3} \quad . \tag{17}$$

In this case, the wall resistance has been eliminated from the composite coefficient by the use of Eq. (9). The abscissa is the liquid film Reynolds number:

$$Re = 4\Gamma/\mu \quad , \tag{18}$$

where Γ is the condensate mass flow rate at bottom of tube per unit length of periphery. All fluid properties (k, ρ, and μ) were evaluated at the equivalent film temperature as suggested by McAdams [3].

As illustrated in Fig. 7, the smooth-tube data lie considerably above the Nusselt [2] (analytical) prediction; however, the semiempirical correlation of McAdams [3] is in good agreement with the smooth-tube data. A correlation by Zazuli [4], which purports to account for ripple effects in the condensate film, seems to be slightly higher than the experimental data on the average. In general, however, it can be claimed that the smooth-tube data are in good agreement with standard correlations.

The smooth-tube data for ammonia are plotted in Fig. 8 along with similar data taken previously at Oak Ridge National Laboratory [12] for fluorocarbons condensing on smooth tubes. The data from all fluids, including ammonia, are seen to group in a rather tight band despite the rather wide spread in individual fluid properties (see Table 3); this suggests that the nondimensional groups account adequately for the governing mechanisms of heat transfer. As seen in Fig. 8, the data for ammonia (squares) span the Reynolds number range of 150 to 1500 and do not enter the laminar-turbulent transition as do the data for the fluorocarbons (Re = 400 to $\sim$3000).

Results from the Wilson plots for the smooth tube were compared with the results using water-side correlations (McAdams, Colburn, and Sieder and Tate) in Eq. (16). The composite condensing coefficients (h^*) from Eq. (16) were in good agreement (-11.4 to +6.9%) with the corresponding Wilson-plot coefficients. The results were not very sensitive to the correlation used for predicting water-side coefficients; thus, the comparison ranged from -10 to 0% with the McAdams correlation, from -6.4 to +6.9% with Colburn, and from -11.4 to 0% with Sieder and Tate. The agreement between the two methods is very good, since $\pm$10 to $\pm$30 is usually considered an acceptable range for predicted heat transfer coefficients.

Fluted Tube

Heat transfer data for the three fluted tubes (E, F, and G) are presented along with smooth-tube (A) data in dimensional form in Fig. 6. More scatter is observed in the fluted-tube data than was found with the smooth-tube data; this difference results from the problems of measuring the lower temperature differences associated with the higher coefficients for the fluted tubes. The coefficients are reported as composite coefficients because of the difficulty in accounting for the wall resistance of the fluted tubes; therefore, it is not convenient to put the coefficients in nondimensional form as was done for the smooth tube. The wall resistance of the smooth tube can be evaluated and is only about 10% of the composite resistance; but for the fluted tubes, the wall resistance is a much greater percentage since the coefficients are significantly higher. Thus, reporting composite coefficients circumvents the problem of evaluating the wall resistance. In practice, designers can work easily with the composite coefficient.

The curves drawn through the experimental data in this section provide only a means for visual comparison and a basis for estimating enhancement ratios; no analytical curve fitting was employed. The data for Tube A in Fig. 6 show

that for a smooth tube heat transfer coefficients decrease only slightly with increasing heat flux in the test range. In contrast, the data for the fluted tubes indicate heat transfer coefficients that are not only considerably higher than those achieved with Tube A but also decrease rapidly with increasing heat flux. Tube E data are slightly above Tube G data at the lower heat fluxes but approach Tube G values at higher heat fluxes ($\sim$11,000 to 12,000 Btu/hr·ft^2). Heat transfer coefficients for Tube F are higher than those for Tube E over the full heat flux range of these experiments. While Tubes E and G have significantly greater condensing area (see Table 1) than Tubes A and F, this effect is essentially accounted for since the ordinate and abscissa bases are on total area bases. Therefore, some additional effect must account for the observed performance improvement. Such results are consistent with those of previous investigators (working primarily with water) who attributed their findings to surface tension drainage effects on contoured surfaces [1,6,8-12]. Alternatively, the condensing coefficient and heat flux can be based on the area determined from the nominal outside (rubber band) tube circumference in which case an improvement in the heat transfer coefficient due to the extra area would also show up.

A comparison of the data for the fluted tubes in Fig. 6 suggests that the heat transfer coefficients are a function of the shape of the flute as well as the size and number of flutes. Thus, the coefficients for Tube E (60 square ridges) are lower than those for Tube F (48 corrugations) and comparable to the coefficients for Tube G (24 corrugations). This suggests that the corrugations or rounded flutes on Tubes F and G are more efficient than square ridges, since fewer flutes are required to achieve better or similar performance. It is observed that the performance of the fluted tubes is similar to that found with fluorocarbons [11,12] where data were substantially above that of a smooth tube; however, the magnitude of the coefficients are much greater for ammonia ($\sim$5 to 10 times for a smooth tube) and is attributed to superior fluid properties of ammonia (see Table 3).

Figure 9 uses an enhancement ratio [R_{h*} = h* (fluted tube)/h* (smooth tube)] to provide another form of comparison between fluted-tube and smooth-tube coefficients. The ratio is plotted as a function of heat flux. For Tube F, the enhancement ratio (R_{h*}) ranged from 5.0 at high heat flux to over 7.0 at low heat flux; for Tube E, the range was 4.3 to 5.5; and for Tube G, 4.0 to 4.8. The magnitude of the enhancement again varies with both the type of fluted tube and the heat flux.

Another dimensional presentation of the data may be more meaningful for particular design situations. In Fig. 10, the data have been replotted as heat load vs condensing temperature difference. In this form (alternate to the previous total area basis), the designer can take "credit" for the increased area of the fluted tube. Thus, for fixed heat load or condensing temperature difference, enhancement factors can be evaluated. In Fig. 10, it can be seen that the performance rank order of test tubes is switched from the order in Fig. 6; that is, Tube A is still the worst, but Tube E is now the best with Tube F second and Tube G third. It is clear that the relative positions of Tubes E and G improve when compared on the heat load-condensing temperature difference basis, because their total surface areas are greater than those of Tubes A and F.

Figure 11 is an enhancement plot for the fluted tubes where the ratio of condensing temperature differences [$R_{\Delta T^*}$ = ΔT^* (smooth tube)/ΔT^* (fluted tube)] is plotted as a function of heat load. The maximum condensing temperature difference ratio was 9.7 at the lowest heat load for Tube E; the minimum ratio was 4.8 at the highest heat load for Tube G.

In a similar manner, the ratio of heat loads [R_Q = Q (fluted tube)/Q (smooth tube)] can be evaluated at a constant condensing temperature difference. The heat load ratio can be estimated from the curves sketched through the data in Fig. 10. The maximum heat load ratio achieved in these tests was 5.4 occurring with Tube E at a condensing temperature difference of 1.2°F (lowest value reported for Tube A). This indicates that Tube A could accommodate only a heat load of 1800 Btu/hr; whereas, Tube E could handle 9700 Btu/hr at a composite condensing temperature difference of 1.2°F. The minimum heat load ratio was 3.5 occurring at the highest condensing temperature difference (4.4°F) with Tube G.

Wilson-plot results for the fluted tubes with smooth inside surfaces (Tubes E and F) were compared with the results obtained using water-side correlations [Eq. (16)]. The smooth-tube correlations for water-side coefficients were not applicable for Tube G, since it contained irregularities on the inside surface. The composite condensing coefficients from Eq. (16) were in fair agreement (-38 to +11.68%) with the corresponding Wilson-plot coefficients for the fluted tubes; the Colburn correlation gave the best agreement for both Tube E (-17 to +9.7%) and Tube F (-3.1 to +11.6%). In general, the coefficients for Tube F were in better agreement than those for Tube E. While agreement is not within ±12% as with the smooth-tube coefficients, it is fairly good considering the rough nature of the predicted water-side coefficients and the sensitivity of the Wilson-plot results to temperature measurement accuracy.

Tube Length Effects

Figure 12 shows a comparison between the heat transfer data for Tube F (4 ft long) and Tube F-1 ("effectively" 2 ft long). As indicated in the figure, the effect of tube length on performance is not detectable. The data for Tube F-1 fall within the normal scatter of the data for Tube F. Present work at Oak Ridge National Laboratory with fluorocarbons has indicated significant effects of tube length on heat transfer performance with shorter condensing lengths improving the heat transfer performance. The decrease in heat transfer performance for longer condensing lengths is attributed to liquid flooding of the drainage channels or troughs. However, the large latent heat of vaporization for ammonia (see Table 3) results in much less condensate and thinner films on the tubes at the same heat flux and could explain why no length effects were observed for tubes of the lengths used in ammonia experiments.

CONCLUSIONS

Heat transfer coefficients for ammonia condensing on the fluted outside surfaces of tubes are up to 7.2 times smooth tube values at a given heat flux; this augmentation cannot be accounted for by the greater surface area of the fluted tubes. These results confirm that fluted tubes, previously shown to enhance steam and fluorocarbon condensing coefficients significantly, are also effective

with ammonia vapors. The magnitude of the heat transfer enhancement varies with both the number of flutes on a tube of given diameter and the heat flux. Rounded flutes (corrugations) appear to be more effective than square flutes (square ridges) for enhancing heat transfer, indicating that the shape of the flute is also a key variable.

For a given heat load, a smooth tube can require condensing temperature differences up to 9.7 times the fluted tube values; conversely, fluted tubes can increase heat load capability up to 5.4 times smooth tube values for a given condensing temperature difference.

No appreciable effect on the heat transfer performance of a fluted tube condensing ammonia was detectable in going from an "effective" condensing length of 4 ft to 2 ft. In this respect the ammonia performance differed substantially from that of the fluorocarbons (for example, R-113), where heat transfer coefficients increased by up to 60% as the tube length was halved. The experimental equipment used in this investigation limited the heat flux to 16,000 Btu/hr·ft^2. Experiments run at higher heat fluxes would provide more insight into the flooding mechanism for ammonia condensing on fluted tubes. This factor may well account for the lack of any observed effect of tube length on condensing coefficients in the present study.

ACKNOWLEDGMENT

This research was performed at the Oak Ridge National Laboratory operated by the Union Carbide Corporation for the Department of Energy (formerly Energy Research and Development Administration). This study was a part of the general program on Low-Temperature Heat Utilization being performed for the ERDA Division of Solar Energy, Ocean Thermal Energy Conversion Branch. The author wishes to acknowledge the support and suggestions of H. W. Hoffman and the assistance of R. L. Linkous in performing the experimental measurements.

REFERENCES

1. L. G. Alexander and H. W. Hoffman, Improved Heat-Transfer Systems for Evaporators — Performance Characteristics of Advanced Evaporator Tubes for Long-Tube Vertical Evaporators, ORNL/TM-2951 (January 1971).

2. W. Nusselt, "Die Oberflächenkondensation des Wasserdampfes," *Z. Ver. Deutsch. Ing.*, 60, 541, 569 (1916).

3. W. H. McAdams, Heat Transmission, 3d ed., McGraw-Hill, New York, 1954.

4. S. S. Kutateladze, Fundamentals of Heat Transfer, p. 307, Academic Press, New York, 1963.

5. C. G. Kirkbride, "Heat Transfer by Condensing Vapors on Vertical Tubes," *Trans. Am. Inst. Chem. Engrs.*, 30, 170 (1933).

6. R. Gregorig, "Film Condensation on Finely Waved Surfaces with Consideration of Surface Tension," *Zeit. fur ang. Math. u. Physik*, 5, 36 (1954).

7. L. D. Landau and E. M. Lifshitz, Fluid Mechanics, p. 230, Pergman Press, New York, 1959.

8. T. C. Carnavos, "Thin Film Distillation," pp. 205-218 in Proceedings of First International Symposium on Water Desalination, Washington, DC, October 3-9, 1965, Vol. 2, 1967.

9. D. G. Thomas, "Enhancement of Film Condensation Heat Transfer Rates on Vertical Tubes by Vertical Wires," *Ind. Eng. Chem. Fundamentals*, 6, 97 (1967).

10. D. G. Thomas, "Enhancement of Film Condensation Rate on Vertical Tubes by Longitudinal Fins," *Am. Inst. Chem. Eng. J.*, 14, 644 (1968).

11. Energy Division Annual Progr. Rep. Dec. 31, 1975, ORNL-5124, pp. 194-197.

12. Energy Division Annual Progr. Rep. Sept. 30, 1976, ORNL-5250, pp. 208-213.

13. A. P. Kratz, H. J. Macintire, and R. E. Gould, *University of Illinois, Engineering Experimental Station, Bull.* 171 (1927), 196 (1928), 209 (1930).

14. E. E. Wilson, "Basis for Rational Design of Heat Transfer Apparatus," *Trans. Am. Soc. Mech. Engrs.*, 37, 47 (1915).

15. "Properties of Refrigerants," Chap. 14, ASHRAE Handbook of Fundamentals, p. 268, ASHRAE, New York, 1972.

16. Thermophysical Properties of Refrigerants, pp. 145-150, ASHRAE, New York, 1973.

17. Thermodynamic Properties of Refrigerants, pp. 131-150, ASHRAE, New York, 1969.

18. K. O. Beatty, Jr., and D. L. Katz, "Condensation of Vapors on Outside of Finned Tubes," *Chem. Eng. Progr.*, 44(1), 55 (1948).

19. A. P. Colburn, "A Method of Correlating Forced Convection Heat Transfer Data and a Comparison with Fluid Friction," *Trans. Am. Inst. Chem. Engrs.*, 29, 174 (1933).

20. E. N. Sieder and C. E. Tate, "Heat Transfer and Pressure Drop of Liquids in Tubes," *Ind. Eng. Chem.*, 28, 1429 (1936).

21. W. M. Rohsenow and H. Y. Choi, Heat, Mass, and Momentum Transfer, Chap. 10, pp. 237-253, Prentice-Hall, New Jersey, 1961.

22. S. K. Combs, An Experimental Study of Heat Transfer Enhancement for Ammonia Condensing on Vertical Fluted Tubes, ORNL-5356 (in press).

TABLE I. CHARACTERISTICS OF TUBES

Cross section	Tube designation	Inside diameter		Outside perimeter		Outside surface area		Number of flutes
		cm	(in.)	cm	(in.)	m^2	(ft^2)	
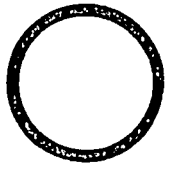	A	2.21	(0.87)	7.98	(3.14)	0.0974	(1.05)	—
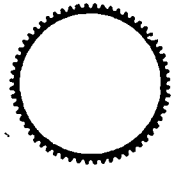	E	2.21	(0.87)	12.70	(5.00)	0.1490	(1.60)	60
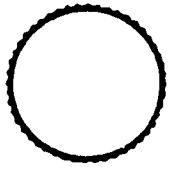	F	2.29	(0.90)	8.26	(3.25)	0.0964	(1.04)	48
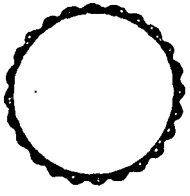	G	2.54	(1.00)	9.75	(3.84)	0.1143	(1.23)	24

TABLE II. PARAMETER RANGES FOR CONDENSING TESTS

Parameter	Units		Test tube A	E	F	F-1	G
Condensing temperature	K	→	293–316	296–314	298–315	301–315	302–316
	(°F)	→	(69–109)	(73–105)	(77–107)	(82–108)	(83–109)
Condensing pressure	MPa	→	0.88–1.7	0.95–1.6	1.0–1.6	1.1–1.6	1.1–1.7
	(psia)	→	(127–242)	(138–227)	(146–236)	(160–240)	(163–245)
Composite condensing temperature difference	K	→	0.7–12.6	0.2–1.8	0.2–2.2	0.2–1.9	0.3–2.5
	(°F)	→	(1.2–22.7)	(0.3–3.2)	(0.4–4.0)	(0.4–3.5)	(0.5–4.4)
Heat load	W	→	500–5000	1000–5000	1000–4800	1050–4500	1000–5100
	(Btu/hr)	→	(1700–17,000)	(3500–17,000)	(3500–16,000)	(3600–15,000)	(3500–17,000)
Heat flux	W/m^2	→	5200–52,000	7000–33,000	11,000–50,000	11,000–48,000	8800–45,000
	($Btu/hr \cdot ft^2$)	→	(1600–16,000)	(2200–11,000)	(3400–15,000)	(3500–15,000)	(2800–14,000)
Composite condensing heat transfer coefficient	$W/m^2 \cdot K$	→	4100–7900	17,000–41,000	22,000–54,000	24,000–48,000	18,000–36,000
	($Btu/hr \cdot ft^2 \cdot °F$)	→	(720–1400)	(3000–7200)	(3900–9600)	(4200–8500)	(3200–6300)

TABLE III. COMPARISON OF FLUID PROPERTIES AT 38°C (100°F)

Property[a]	Units		Refrigerant number (Formula)					
			11 (CCl_3F)	21 ($CHCl_2F$)	22 ($CHClF_2$)	114 ($C_2Cl_2F_4$)	717 (NH_3)	718[b] (H_2O)
Saturation pressure, P_{sat}	Pa	→	1.618×10^5	2.761×10^5	1.452×10^6	3.161×10^5	1.461×10^6	6550
	(psia)	→	(23.46)	(40.04)	(210.6)	(45.85)	(211.9)	(0.950)
Thermal conductivity, k	W/m·K	→	0.0839	0.0974	0.0815	0.0613	0.452	0.628
	(Btu/hr·ft·°F)	→	(0.0485)	(0.0563)	(0.0471)	(0.0354)	(0.261)	(0.363)
Viscosity, μ	Pa·s	→	3.70×10^{-4}	2.84×10^{-4}	1.84×10^{-4}	2.9×10^{-4}	1.23×10^{-4}	6.53×10^{-4}
	(lb_m/hr·ft)	→	(0.894)	(0.686)	(0.0444)	(0.71)	(0.298)	(1.58)
Density, ρ	kg/m^3	→	1445	1335	1141	1416	583.1	993.2
	(lb_m/ft^3)	→	(90.21)	(83.36)	(71.23)	(88.40)	(36.40)	(62.00)
Latent heat of vaporization, h_{fg}	J/kg	→	1.749×10^5	2.211×10^5	1.693×10^5	1.230×10^5	1.110×10^6	2.410×10^6
	(Btu/lb_m)	→	(75.24)	(95.12)	(72.84)	(52.91)	(477.8)	(1037)
Heat capacity, c_p	J/kg·K	→	895	1090	1310	1040	4845	4175
	(Btu/lb_m·°F)	→	(0.214)	(0.260)	(0.313)	(0.249)	(1.158)	(0.998)
Surface tension, σ	N/m	→	0.0167	0.0163	0.00645	0.0105	0.0175	0.0699
	(lb_f/ft)	→	(1.14×10^{-3})	(1.12×10^{-3})	(4.42×10^{-4})	(7.20×10^{-4})	(1.20×10^{-3})	(4.79×10^{-3})

[a]The properties k, μ, ρ, and c_p are for the liquid.

[b]Shown for comparison.

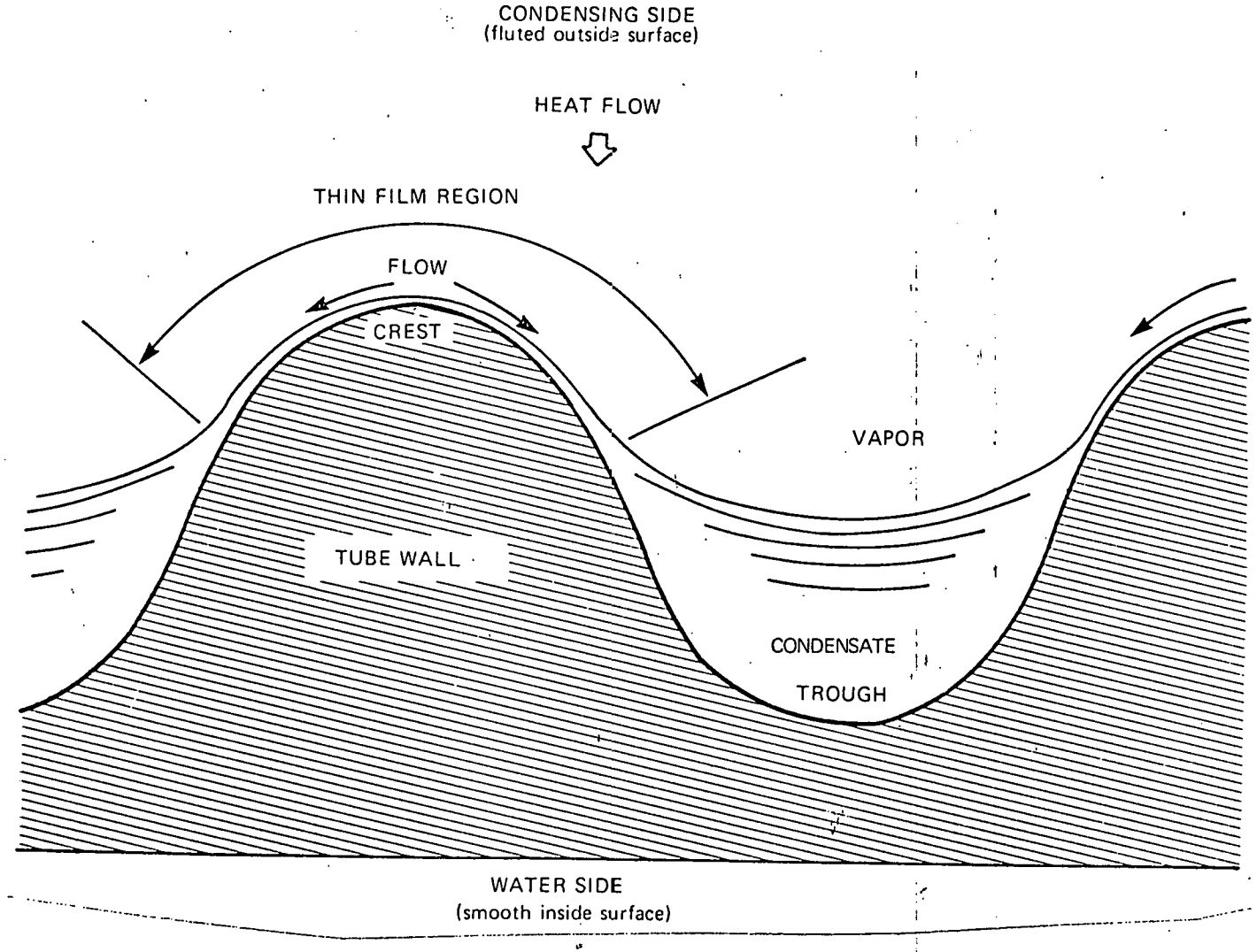

Fig. 1. Fluted Tube Principle of Operation (Condensation Mode) — Surface Tension Forces Acting to Push Condensate from Crests in Troughs.

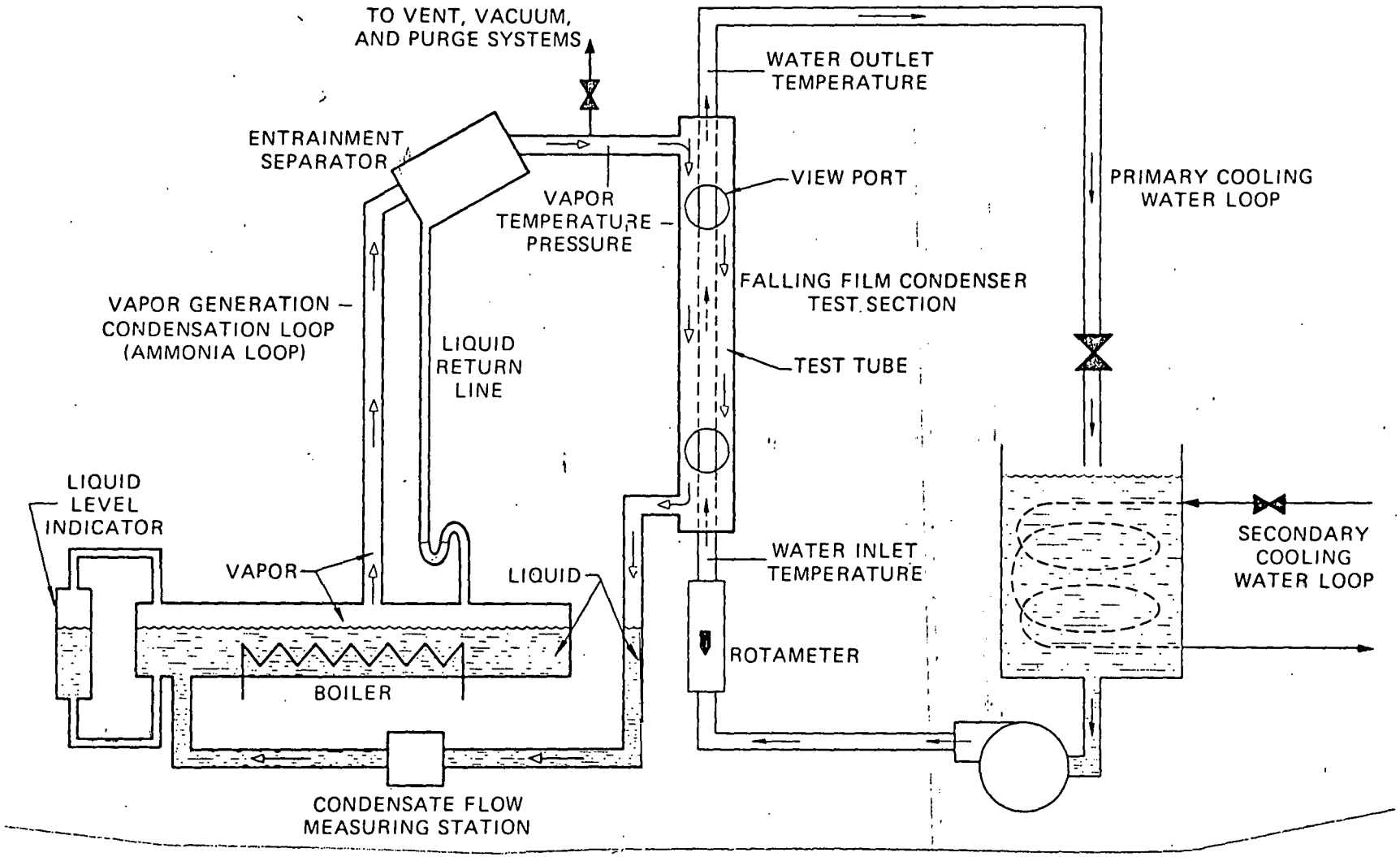

Fig. 2. Schematic Diagram of Experimental Apparatus.

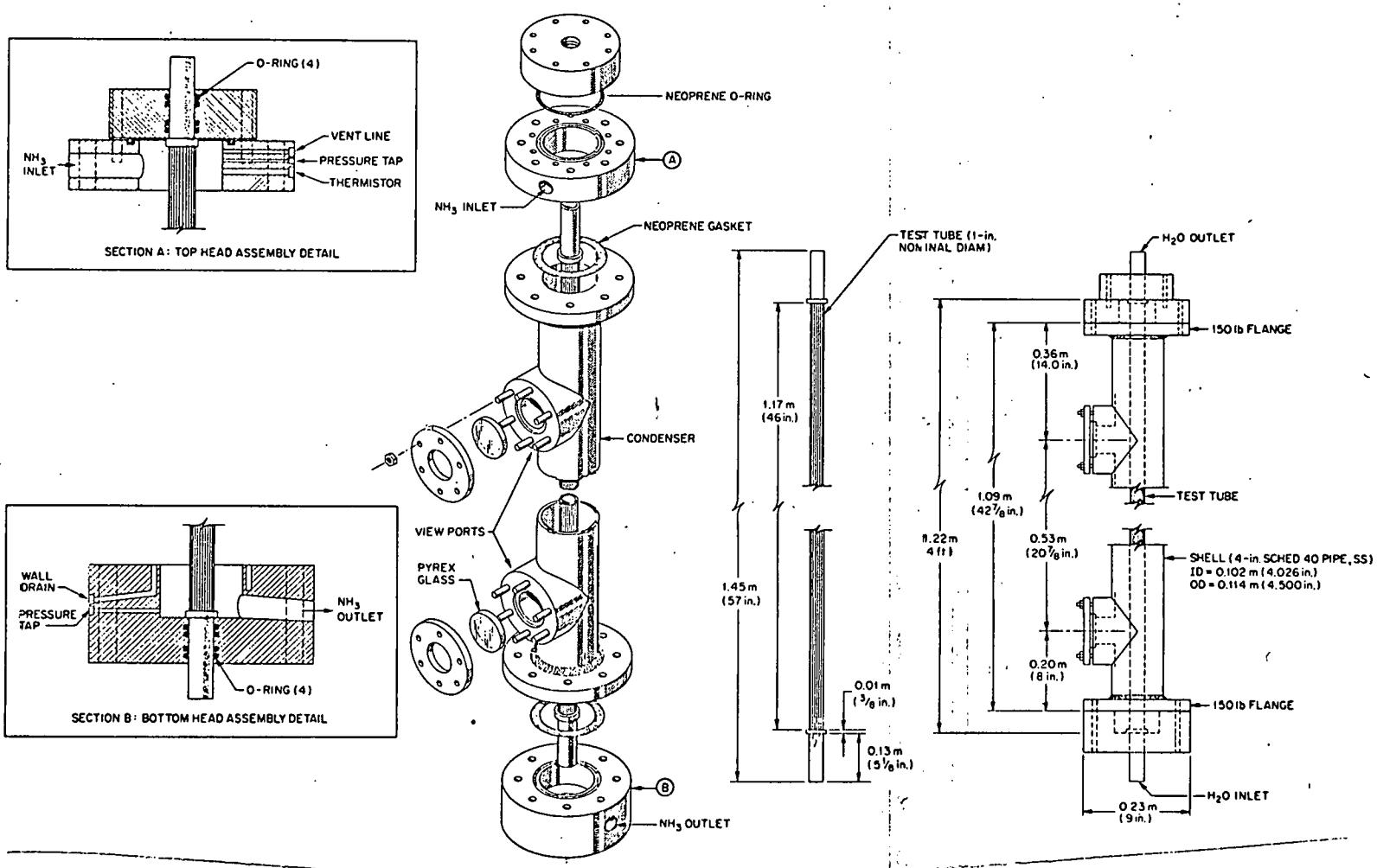

Fig. 3. Details of the Test Section.

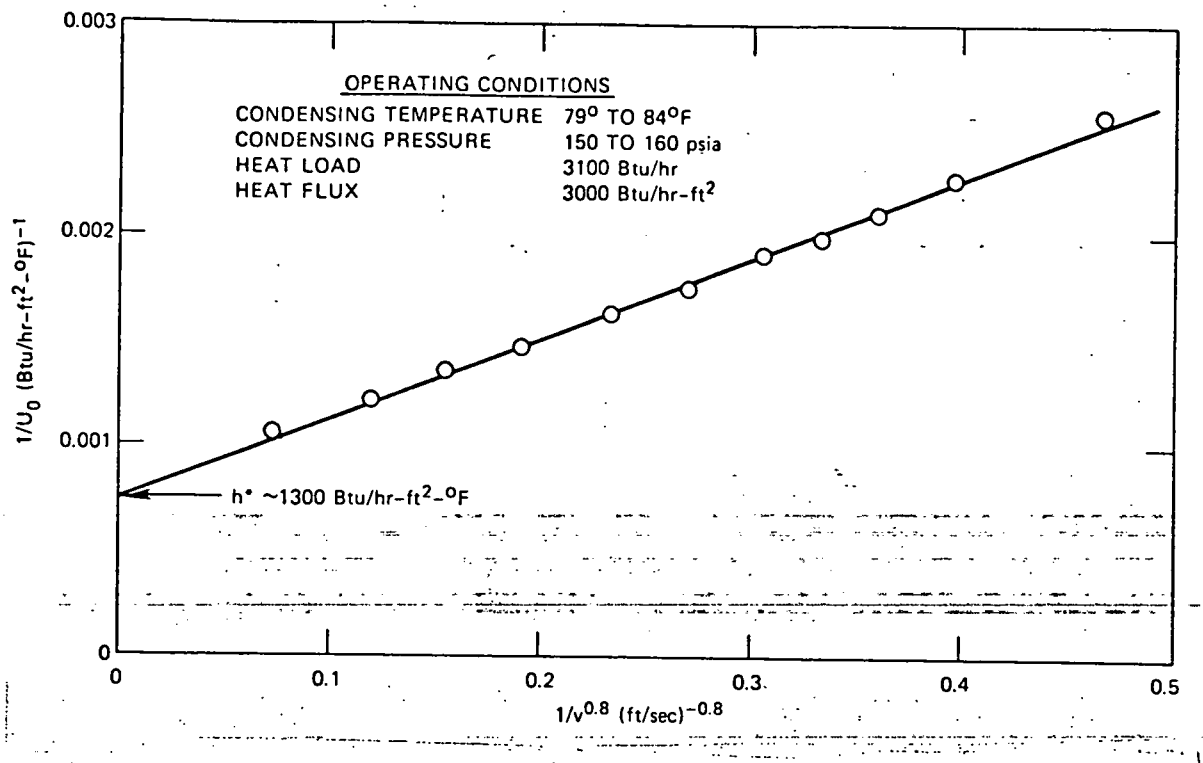

Fig. 4. Wilson Plot for Ammonia Condensing on Tube A (Smooth Tube).

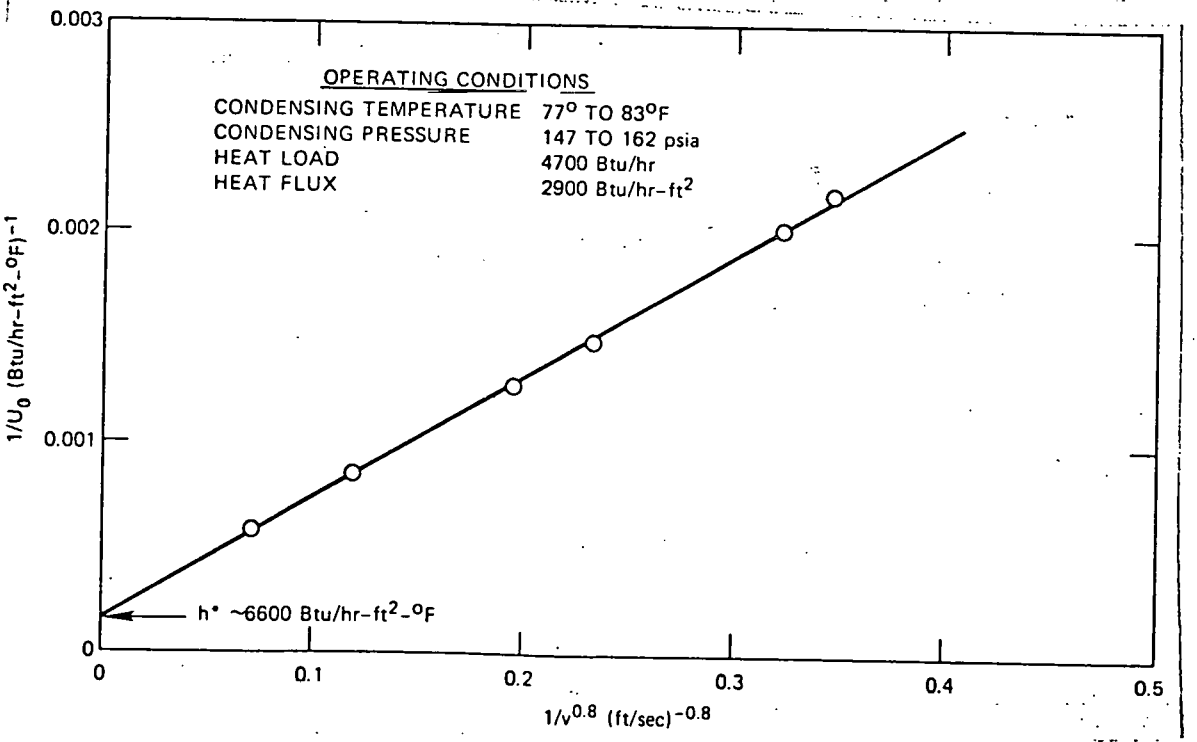

Fig. 5. Wilson Plot for Ammonia Condensing on Tube E (60 Square Ridges).

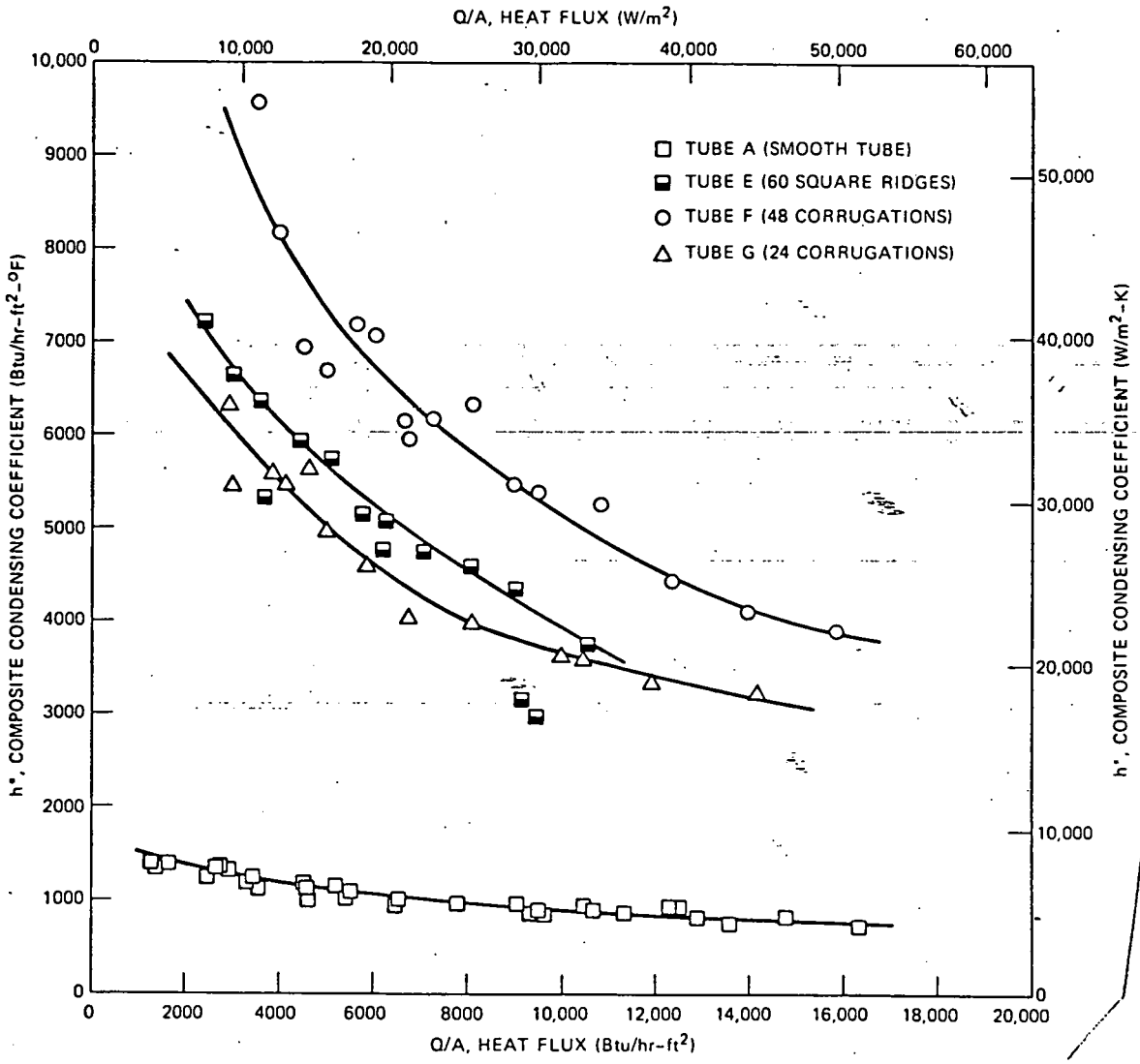

Fig. 6. Composite Condensing Heat Transfer Coefficients for Ammonia.

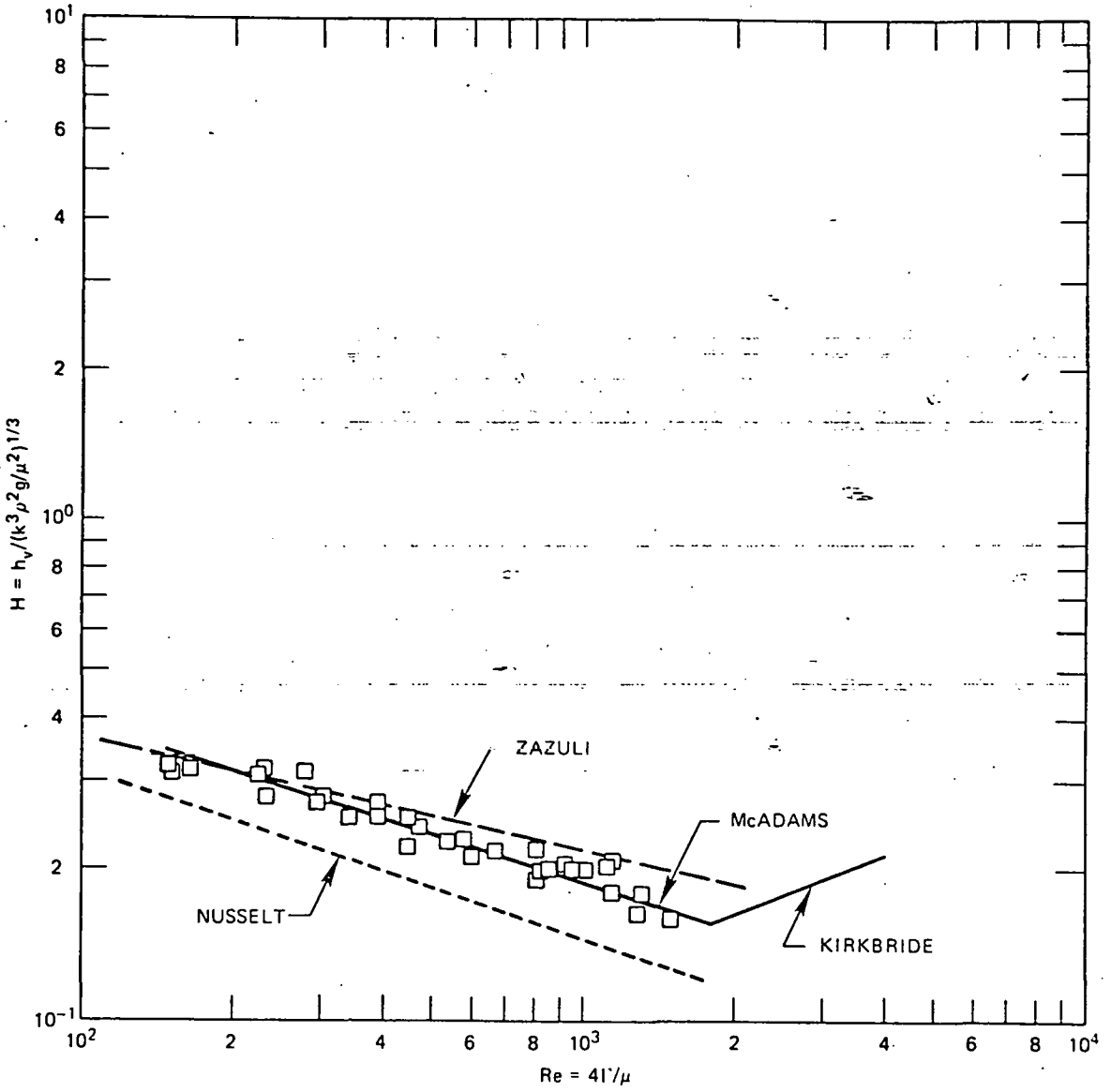

Fig. 7. Vertical Smooth-Tube (A) Condensation Data for Ammonia — Standard Nondimensional Coordinates.

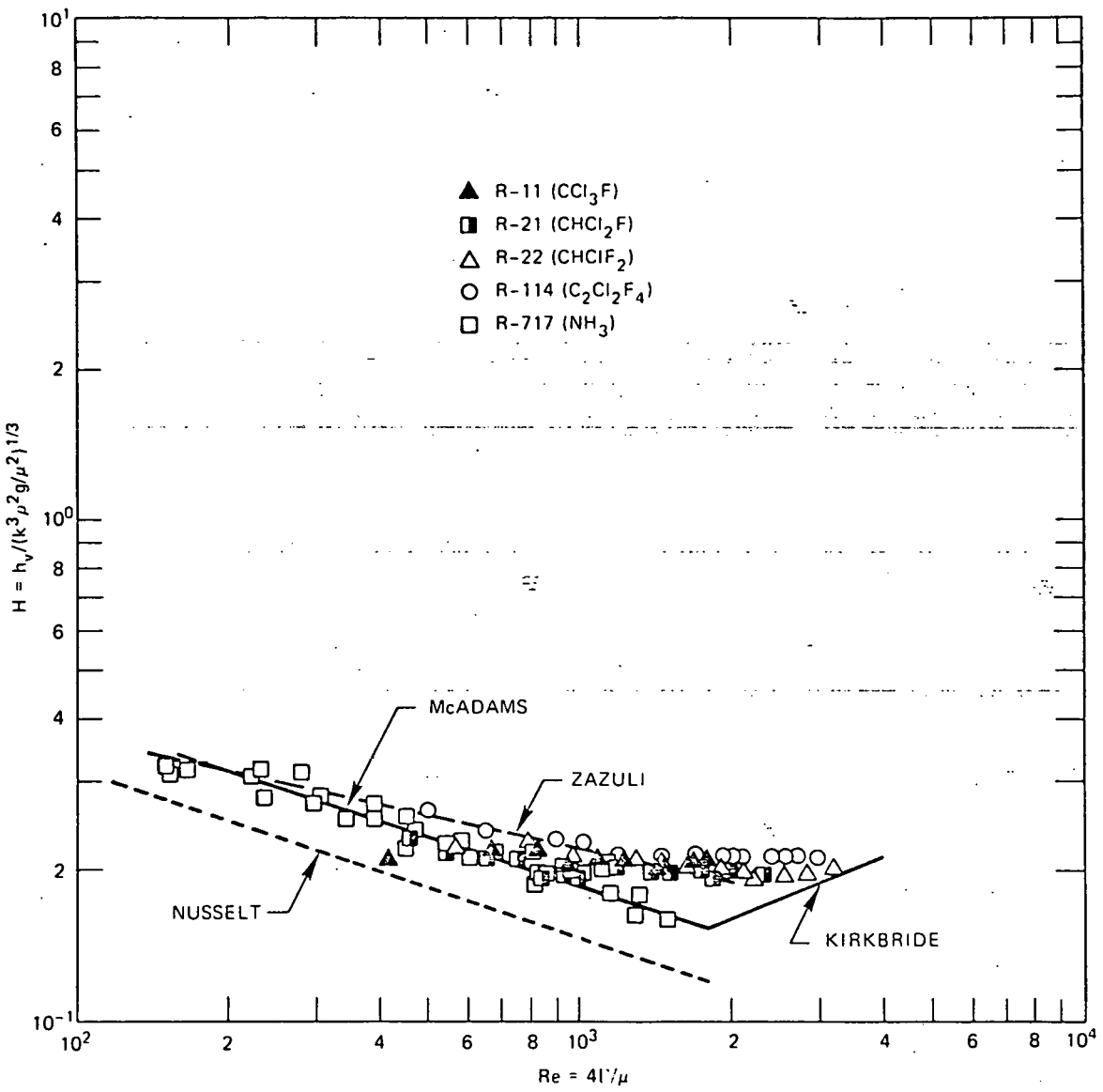

Fig. 8. Comparison of Vertical Smooth-Tube (A) Condensation Data for Ammonia to Similar Data for Fluorocarbons — Standard Non-dimensional Coordinates.

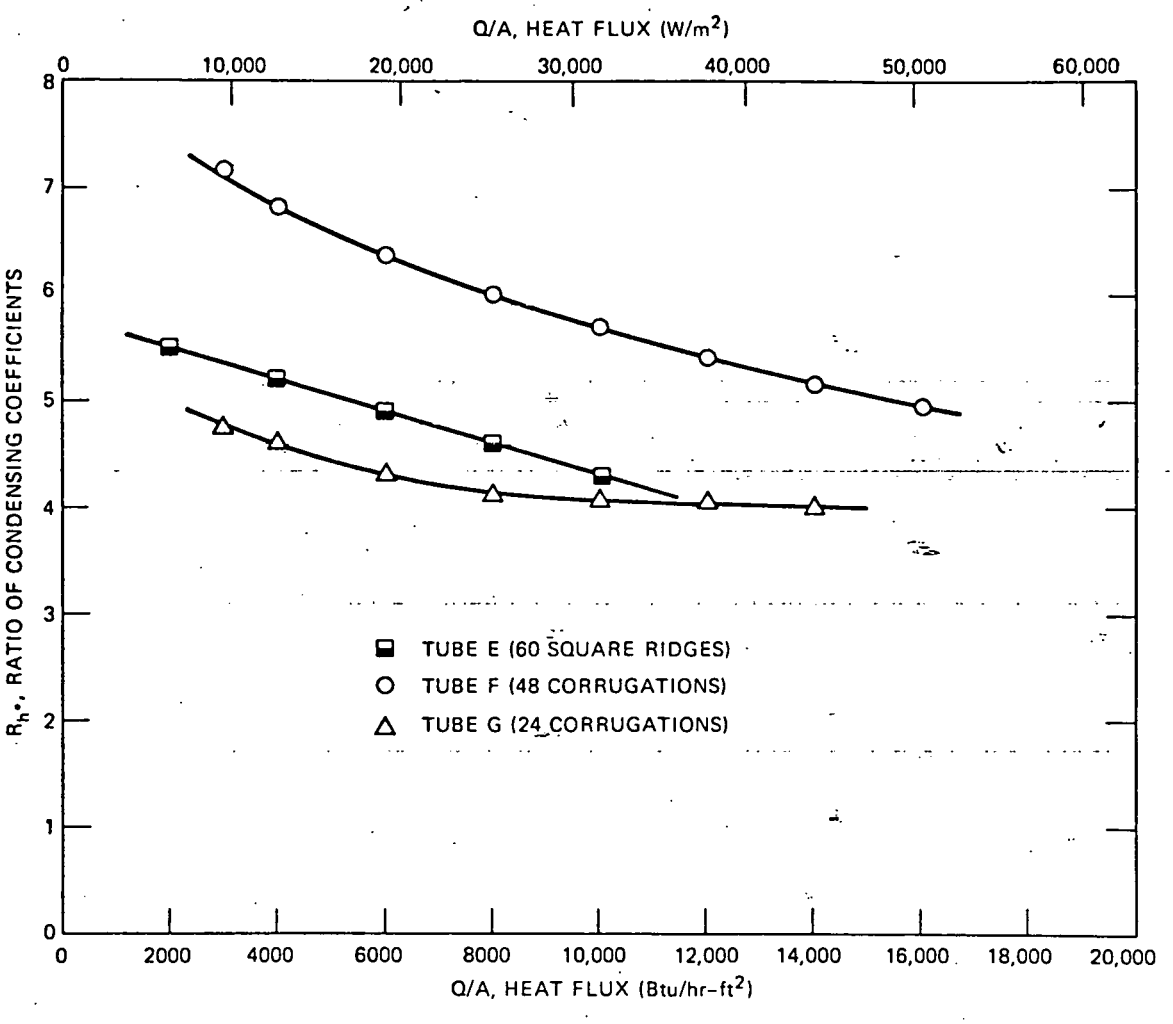

Fig. 9. Fluted-Tube Heat Transfer Enhancement Plot for Ammonia — Ratio of Condensing Coefficients [R_{h*} = h* (Fluted Tube)/h* (Smooth Tube)] vs Heat Flux.

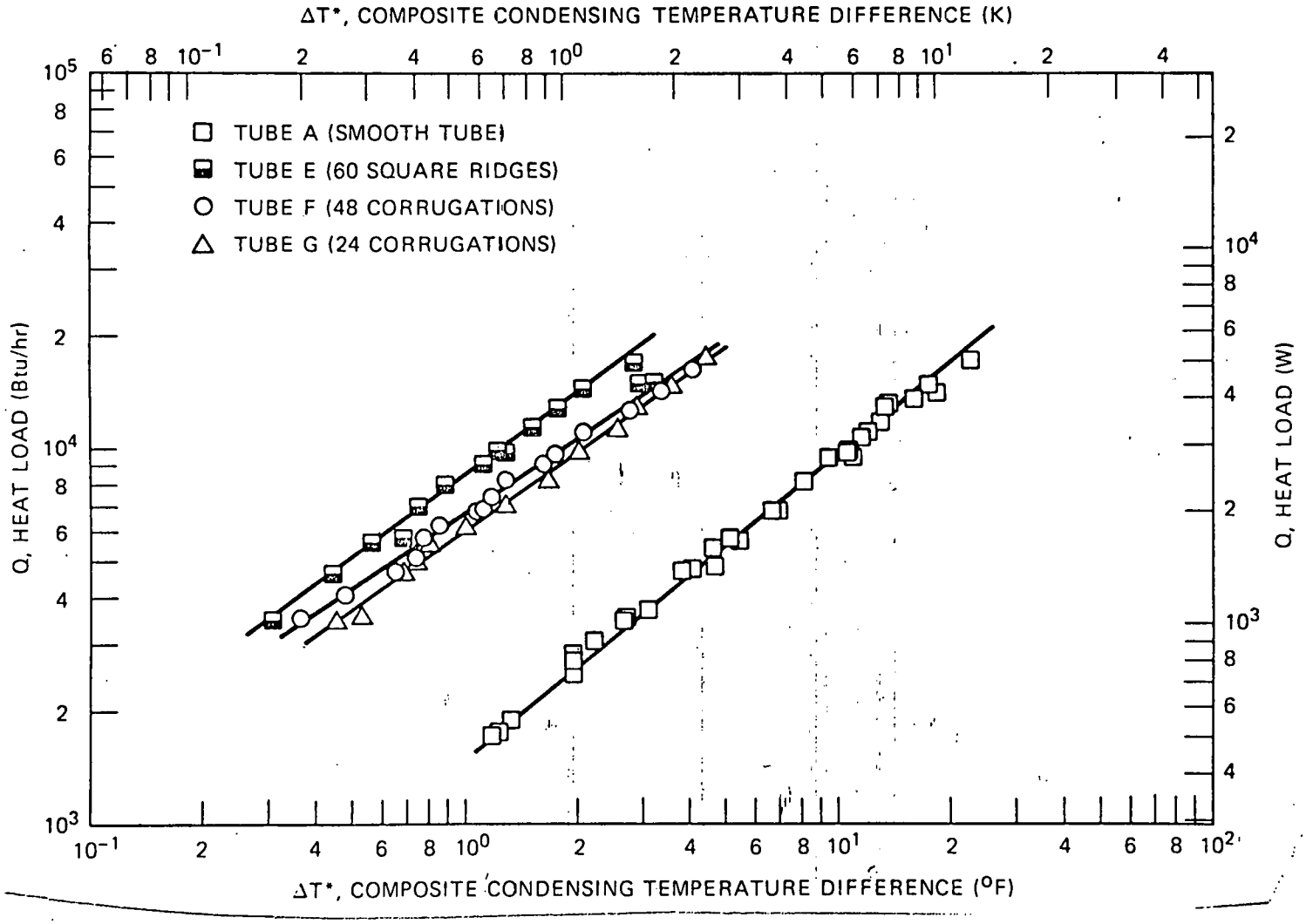

Fig. 10. Heat Load vs Composite Condensing Temperature Difference for Ammonia.

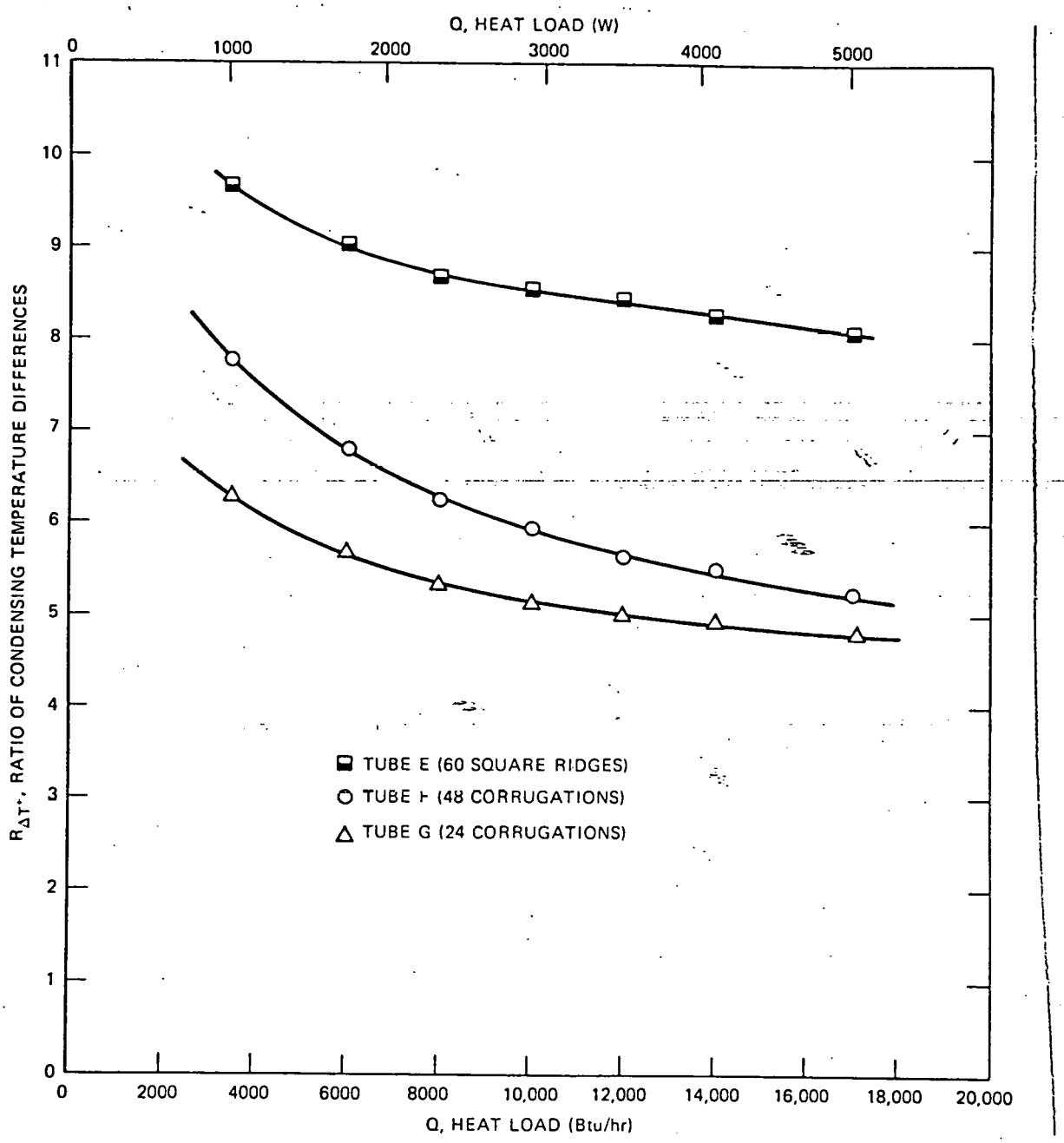

Fig. 11. Fluted-Tube Heat Transfer Enhancement Plot for Ammonia — Ratio of Condensing Temperature Differences [$R_{\Delta T^*}$ = ΔT^* (Smooth Tube)/ ΔT^* (Fluted Tube)] vs Heat Load.

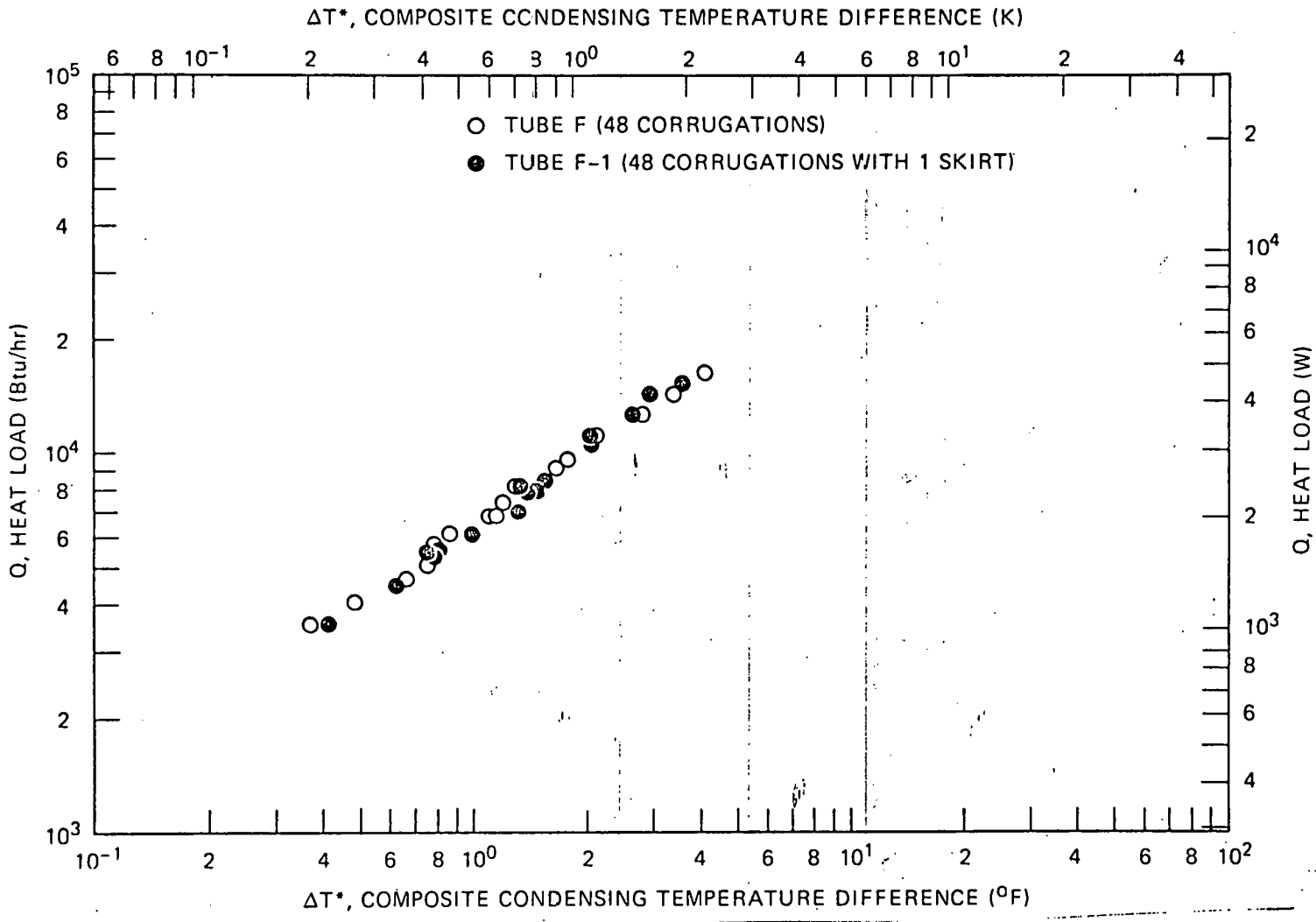

Fig. 12. Comparison of Heat Transfer Performance Between Tube F (48 Corrugations) and a Duplicate Tube (F-1) Containing a Skirt at Midpoint of the Condensing Length — Q vs ΔT*.